Chapter 6

Dynamic Rheological Properties

This chapter is mainly centred on the rheological properties of PP/HDPE blends. The rheological properties of both compatibilised and uncompatibilised blends are discussed in detail. The most important feature of this chapter is that we calculated interfacial tension between the polymers from the storage modulus of the blends using two well-known models, viz. Palierne and Choi-Schowalter. The effect of compatibilisation on the interfacial tension between the polymers is discussed. Attempts are also made to correlate the phase morphology with rheology.

The results of this chapter have been submitted for publication in Polymer

6.1. Introduction

Nowadays dynamic rheological measurements have received much attention as an extremely powerful rheological technique, which offers several advantages over the conventional steady shear rheometry because of its unique ability to assess and provide important informations on the frequency dependence of rheological properties and on the physical and microstructure of materials without disturbing the conformation of the material appreciably. In this technique, a sinusoidally varying strain is imposed on the polymeric material and the resulting stress may be separated into pure elastic and viscous responses from which useful informations on the melt rheology and processing characteristics can be obtained.

The rheological properties of molten components in immiscible polymer blends affect the processing/morphology/ property relationships [1-5]. The classic theory of rheology of emulsions focuses on dilute emulsions of spherical, Newtonian drops; see e.g. Frankel and Acrivos [6] and Schowalter et al. [7]. A cell theory for more concentrated emulsions has been reported by Palierne [8] that applies to dynamic shear with very small drop deformation from a spherical shape. Other computational results on concentrated emulsion rheology have been presented by Loewenberg and Hinch [9] for shear flows with appreciable departures from a spherical shape for the dispersed phase. The Palierne theory has an added distinction of being formulated for viscoelastic constituents. Two other models of emulsion rheology have been applied widely to polymer blends in the dilute and semi dilute regimes to explain their rheological behaviour are due to Oldroyd [10] and Choi and Schowalter, [11] respectively.

The rheology and morphology of multiphase polymer blends are strongly affected by interfacial characteristics. Several models have been proposed to describe either the influence of compatibilisers on the deformation of dispersed phase or to derive rheological parameters such as the complex shear modulus (G*), the storage modulus (G') and the loss modulus (G") [8,11-21]. Palierne model has widely been employed to depict the rheological response of various blend systems [22-32]. Friedrich et al. [33] reported that the particle size distribution can be derived from measured data if the interfacial tension is known. On the other hand, interfacial

tension can also be estimated from particle size distribution using the Palierne model as shown by Asthana et al. [25] and Shi et al. [26]. Also, micro-mechanical models, such as that of Coran and Patel [34] which reflects the morphology, together with the common series and parallel mixing rule approaches, have been found to be appropriate to describe the observed rheological response [35].

Jafari et al. [36] investigated the morphology and rheology of poly(trimethylene terephthalate)/metallocene linear low-density polyethylene (PTT/m-LLDPE) immiscible blends with varying extent of compatibilisation and theoretically analyzed using Palierne and Coran models. Rheological examinations showed a sharp reduction of complex viscosity for the latter system at 10wt% compatibiliser which is ascribed to the micelle formation in the bulk phase. Plots of the relaxation time spectrum exhibit that upon addition of the compatibiliser the magnitude of the relaxation peaks associated with interface increases which is attributed to the increase of the interfacial area. The Palierne model failed to predict admissible values and reasonable trend for interfacial tension. This failure is believed to be due to the excessively large difference between the complex shear modulus values of the dispersed and matrix phases.

The present chapter is devoted to study the rheological properties of PP/HDPE blends in the presence and absence of compatibilisers. Dynamic rheological method using a plate/plate rheometer has been employed to evaluate the viscoelastic properties such as storage and loss moduli, complex viscosity, etc. of uncompatibilised and compatibilised blends. Further, we tried to correlate the phase morphology with rheological data. Finally, the experimental results were compared with different models, such as Palierne model and Choi-Schowalter model.

6.2. Results and discussion

6.2.1. Uncompatibilised blends

Effect of blend ratio on the complex viscosity of uncompatibilised PP/HDPE blends is given in Fig. 6.1. As the frequency increases, the complex viscosity decreases. Further, with increase in frequency, the relaxation time decreases or in other words, the shear rate increases. Thus an increase in frequency has the same effect as that of increase in shear rate. Thus in all cases, pseudoplastic behaviour

is seen. It is seen from the figure that PP has the maximum while HDPE has the minimum complex viscosity in the whole range of frequency. However, as the frequency increases, the difference between the viscosities of two polymers decreases. The complex viscosity of all the blends is found to be intermediate between the neat polymers in such a way that addition of HDPE into PP decreases the complex viscosity (even though some discrepancies are seen at higher frequencies). It should be noted that the viscosity difference between the polymers has significant impact on the phase morphology of the blends. If the minor component has lower viscosity compared to the major one, it will be finely and uniformly dispersed in the major continuous phase owing to the diffusional restrictions imposed by the matrix [37] and otherwise coarsely dispersed. It is believed that viscosity ratio should be approximately unity when designing the polymer blends for superior properties.

Wu's equation (equation 6.1) suggests that minimum particle size is achieved when the viscosities of the two phases are closely matched and as the viscosity moves away form unity in either direction, the dispersed particles become larger [38].

$$D = \frac{4\Gamma\lambda^{\pm 0.84}}{\dot{\gamma}\eta_m} \qquad (6.1)$$

where D is the droplet diameter η_m the viscosity of the matrix, p the viscosity ratio of the droplet phase to the matrix, $\dot{\gamma}$ the shear rate and Γ the interfacial tension.

We observed a similar result since the phase morphology of PP/HDPE blends (chapter 3) revealed that for a given composition of minor component, the relatively less viscous HDPE forms smaller dispersed droplets in more viscous PP matrix phase. At the same time there is no big difference between the viscosities of the two polymers as seen in Table 6.1 which presents the viscosity ratio of the polymers at selected frequencies. Thus one can expect no considerable difference between the phase morphologies of PP rich and HDPE blends and a co-continuous morphology in the range 40 to 60wt% of one of the components. All these facts are found to be true in PP/HDPE system and thus it can be argued that there is perfect correlation between the morphology and rheology of uncompatibilised PP/HDPE blends.

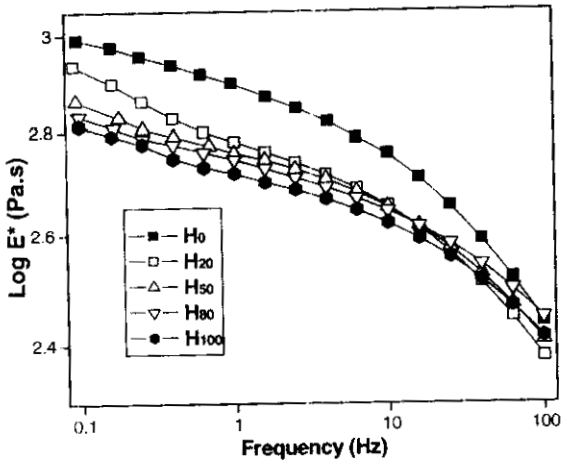

Figure 6.1: Effect of blend ratio on the complex viscosity of uncompatibilised PP/HDPE blends

Figures 6.2 and 6.3 show the effect of blend ratio on the storage and loss moduli of uncompatibilised PP/HDPE blends. Both storage and loss moduli show same trend, i.e., increase with increase in frequency. This is not unexpected since with increase in frequency, polymer chains get less relaxation time and consequently moduli increased. It is also important to note that unlike complex viscosity (property of viscous phase of polymer), modulus values (property of elastic phase) are higher for HDPE.

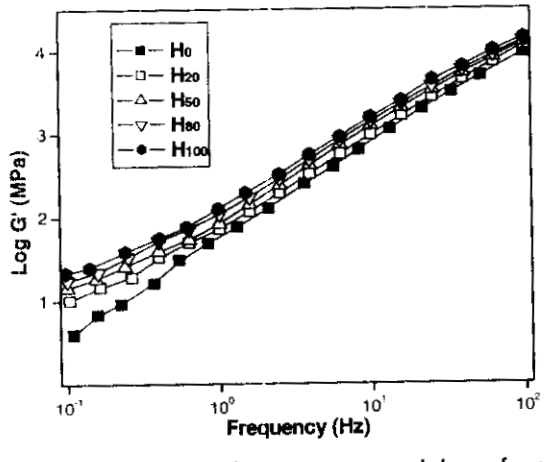

Figure 6.2: Effect of blend ratio on the storage modulus of uncompatibilised PP/ HDPE blends

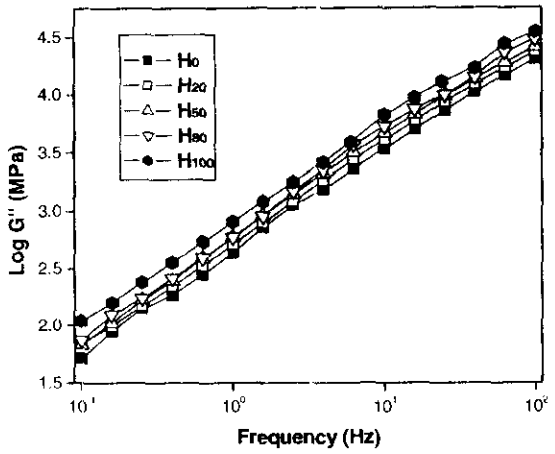

Figure 6.3: Effect of blend ratio on the loss modulus of uncompatibilised PP/HDPE blends

Frequency (Hz)	Complex viscosity (η) Pa.s		Viscosity ratio
	PP	HDPE	(η_{PP}/η_{HDPE})
0.1	979	649	1.51
0.25	903	597	1.51
0.5	844	544	1.55
1	790	521	1.51
2.5	704	487	1.44
5	636	452	1.41
10	568	417	1.36
25	452	360	1.26
50	360	310	1.16
100	275	259	1.06

Table 6.1: Viscosity ratio of PP and HDPE at various frequencies

6.2.2. Compatibilised blends

Figure 6.4 shows the effect of compatibilisation on the complex viscosity of H_{20} blends. Complex viscosity increases with the addition of compatibiliser in the whole frequency range. The increase in complex viscosity is taken as an evidence for the compatibilising action of EPDM. Increase in complex viscosity with increase in compatibiliser concentration was reported by Brahimi et al. [15], Macaubas et al. [39], and Kim and co-workers [40] for PE/PS blends

compatibilised with (styrene-butadiene (SB) diblock copolymer, PP/PS compatibilised with triblock copolymer, styrene-butadiene-styrene (SBS) and polystyrene/styrene acrylonitrile (PS/SAN) blends compatibilised with PS-g-SAN graft copolymer, respectively. However in contrary to the expectation based on phase morphology that complex viscosity will level off or decrease beyond CMC, it is seen that there is no levelling off in complex viscosity at higher compatibiliser concentration. Blends with 20wt% compatibiliser exhibited maximum complex viscosity. But it can also be seen that beyond, 5wt% compatibiliser concentration, the rate of increase is relatively small. The increase in complex viscosity at higher compatibiliser concentration may be attributed to the high viscosity of the compatibiliser since beyond 5wt% (CMC), EPDM random copolymer forms micelle and therefore contribute to the total viscosity of the system. The decrease in the rate of enhancement of viscosity also justifies this argument. Thus the increase in viscosity beyond 5wt% compatibiliser addition may not be strictly due to compatibilising action of the copolymer.

The effect of compatibilisation on the storage and loss moduli is shown in Figs. 6.5 and 6.6, respectively. From the figures, it is obvious that addition of compatibiliser increases the moduli. The rate of increase is high up to CMC and beyond that levelling off is seen. The pronounced elastic properties in the presence of compatibiliser are mainly due to the enhanced interfacial adhesion with the incorporation of compatibiliser. Dynamic rheological properties of H_{50} compatibilised blends also demonstrate similar results. For example, the complex viscosity of the blends increased in the presence of compatibiliser as seen in Fig. 6.7. Thus it can be concluded that compatibilisation increased the dynamic rheological properties of the blends upto CMC and beyond that there is only marginal increase in properties. Thus the rheological properties in the presence of compatibilisers are also in correlation with the phase morphology.

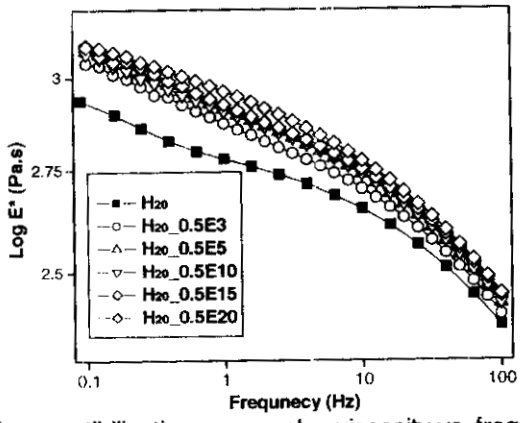

Figure 6.4: Effect of compatibilisation on complex viscosity vs. frequency for H_{20} blends

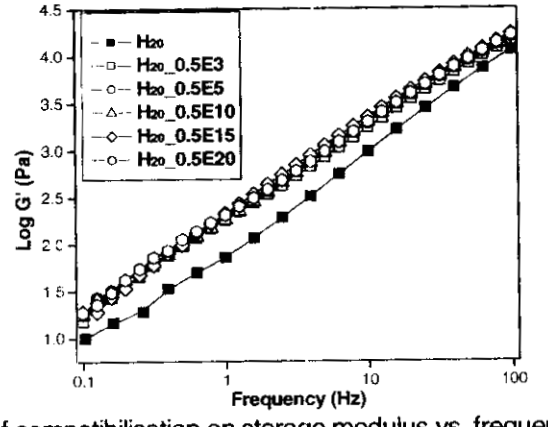

Figure 6.5: Effect of compatibilisation on storage modulus vs. frequency for H_{20} blends

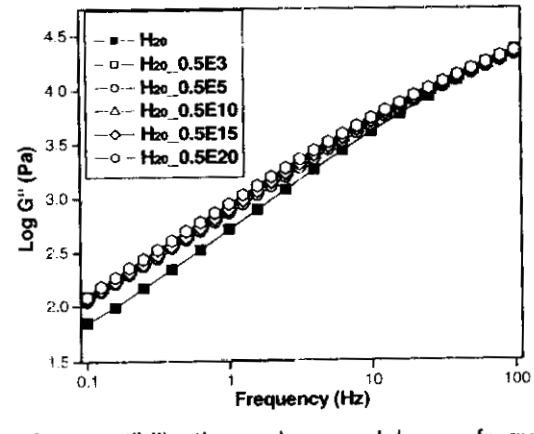

Figure 6.6: Effect of compatibilisation on loss modulus vs. frequency for H_{20} blends

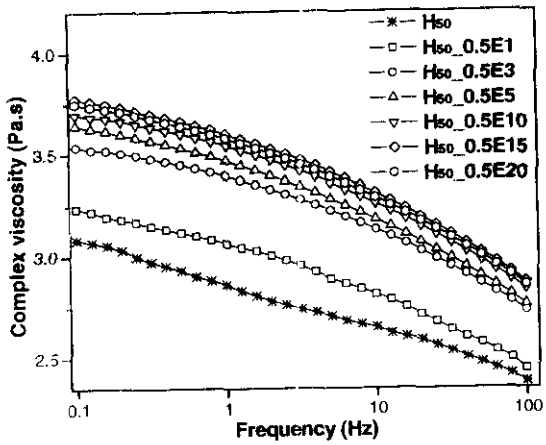

Figure 6.7: Effect of compatibilisation on complex viscosity vs. frequency for H_{50} blends

6.2.3. Palierne model

6.2.3.1. Theoretical basis

Palierne model describes the linear viscoelastic behaviour of emulsions of viscoelastic fluids. It has been shown to be very useful for predicting the rheological behaviour of the immiscible blends [13,15,16,19,41-43]]. The model was used to determine the interfacial tension between the components [13,44], to determine the volume average radius of the dispersed particles [24], to calculate the sphere-size distribution from rheological data [33], to analyse the deformation of droplets under elongational flow [45]. By analogy with an electric formalism, Palierne derived an equation for predicting the complex modulus of molten (emulsion type) blends (G_b^*), which is a function of the complex moduli of both phases G_m^* (for the matrix) and G_b^* (for the inclusions or dispersed phase) taking into account of several important features of a multiphase system. The viscoelasticity of phases, the hydrodynamics interactions, the droplet size and size distribution and the interfacial tension are indeed included in this formulation.

Jacobs et al. [46] developed an extended form of the Palierne model, written as,

$$G_b^* = G_m^* \frac{1+3\int_0^\infty \frac{E(\omega,R)}{D(\omega,R)} v(R)\,dR}{1-2\int_0^\infty \frac{E(\omega,R)}{D(\omega,R)} v(R)\,dR} \qquad (6.2)$$

in which

$$E(\omega,R)=\left(\left[G_d^*(\omega)-G_m^*(\omega)\right]\left[19G_d^*(\omega)+16G_m^*(\omega)\right]+\frac{4\alpha}{R}\right)$$
$$\mathrm{X}\left[5G_d^*(\omega)-2G_m^*(\omega)\right]+\frac{\beta^{I}(\omega)}{R}\left[23G_d^*(\omega)-16G_m^*(\omega)\right] \quad (6.3)$$
$$+\frac{2\beta^{II}(\omega)}{R}\left[13G_d^*(\omega)-8G_m^*(\omega)\right]+\frac{24\beta^{II}(\omega)\alpha}{R^2}+16\beta^{II}(\omega)\frac{\alpha+\beta^{I}(\omega)}{R^2}$$

and

$$D(\omega,R)=\left[2G_d^*(\omega)+3G_m^*(\omega)\right]\left[19G_d^*(\omega)+16G_m^*(\omega)\right]$$
$$+\frac{40\alpha}{R}\left[G_d^*(\omega)+G_m^*(\omega)\right]+\frac{2\beta^{I}(\omega)}{R}\left[23G_d^*(\omega)+32G_m^*(\omega)\right] \quad (6.4)$$
$$+\frac{4\beta^{II}(\omega)}{R}\left[13G_d^*(\omega)+12G_m^*(\omega)\right]+\frac{48\beta^{I}(\omega)\alpha}{R^2}+32\beta^{II}(\omega)\frac{\alpha+\beta^{I}(\omega)}{R^2}$$

where, $G_b^*(\omega)$, $G_m^*(\omega)$ and $G_d^*(\omega)$ represent complex modulus of blend, matrix and dispersed phase, respectively. $\beta^{I}(\omega)$ and $\beta^{II}(\omega)$ are the complex interfacial dilation and shear moduli, respectively. $\nu(R)$ denotes the particle size distribution function while R, α *and* ω are particle radius, interfacial tension, and strain frequency, respectively. When the deformation of dispersed phase is small enough so that viscoelastic properties remain linear, we can set both $\beta^{I}(\omega)$ and $\beta^{II}(\omega)$ to zero. Graebling et al. [13] by assuming the particle size distribution to be narrow $(R_v/R_n \le 2))$ and interfacial tension to be independent of shear and interfacial area variation, simplified equation as:

$$G_b^*=G_m^*\frac{1+3\Sigma_i\varphi_i H_i(\omega)}{1-2\Sigma_i\varphi_i H_i(\omega)} \quad (6.5)$$

where

$$H_i(\omega)=\frac{(4\alpha/R_i)\left(2G_m^*(\omega)+5G_d^*(\omega)\right)+\left(G_d^*(\omega)-G_m^*(\omega)\right)\left(16G_m^*(\omega)+19G_d^*(\omega)\right)}{(40\alpha/R_i)\left(G_m^*(\omega)+G_d^*(\omega)\right)+\left(2G_d^*(\omega)-3G_m^*(\omega)\right)\left(16G_m^*(\omega)+19G_d^*(\omega)\right)} \quad (6.6)$$

in which, R_i and ϕ_i denote the i[th] particle fraction radius and the i[th] volume fraction of dispersed phase, respectively. The interfacial tension can then be estimated by fitting the experimental data to the Palierne model. Using (α) as fitting parameter, the best fit gives the interfacial tension.

6.2.3.2. Interfacial tension measurements

We calculated the interfacial tension based on the weighted relaxation spectrum ($\tau H_{(\tau)}$) with the relaxation time (τ) for PP/HDPE blends. In order to get the weighted relaxation spectrum the following equations were used:

$$G'_{(\omega)} = \int_{-\infty}^{\infty}\left[\left(H_{(\tau)}\omega^2\tau^2\right)\Big/\left(1+\omega^2\tau^2\right)\right]d\left(\ln\tau\right) \tag{6.7}$$

$$G''_{(\omega)} = \int_{-\infty}^{\infty}\left[\left(H_{(\tau)}\omega\tau\right)\Big/\left(1+\omega^2\tau^2\right)\right]d\left(\ln\tau\right) \tag{6.8}$$

the relaxation spectrum can be determined using Tschoegle approximation [47] as given in following equation:

$$H_{(\tau)} = G'\left\{\begin{bmatrix}\left(d\left(\log G'\right)\Big/d\left(\log\omega\right)\right)- \\ 0.5\left(d\left(\log G'\right)\Big/d\left(\log\omega\right)\right)^2\end{bmatrix}-\begin{bmatrix}(1/4.606)\left[d^2\left(\log G'\right)\Big/d\left(\log\omega\right)^2\right]\end{bmatrix}\right\}_{1/\omega=\tau/\sqrt{2}} \tag{6.9}$$

where ω is the frequency and τ is the relaxation time. It should be noted for neat polymer one will get one relaxation time where as for blends two τ (τ_1 and τ_2) will be there corresponding to the component polymers. The difference in the values $(\tau_1 - \tau_2)$ was used to calculate the interfacial tension between the polymers in the presence and absence of compatibilisers. The interfacial tension (α) was calculated using two methods:

(i) Palierne [8] (equation 6.10 and (ii) Choi-Schowalter [11] (6.11).

$$\alpha = \left[\frac{R_v\eta_m}{4\tau}\right]\left[\frac{(19K+16)(2K+3-2\phi(K-1))}{(10(K+1))-(2\phi(5K+2))}\right] \tag{6.10}$$

$$\alpha = \left[\frac{R_v \eta_m}{\tau}\right]\left[\frac{(19K+16)(2K+3)}{40(K+1)}\right]\left[1+\phi\left(\frac{5(19K+16)}{4(K+1)(2K+3)}\right)\right] \qquad (6.11)$$

where η_m is the viscosity of the matrix, ϕ is the volume fraction of the dispersed phase, K is the viscosity ratio and is given as $K = \eta_d/\eta_m$ (η_d is the viscosity of the dispersed phase). Note that both these equations are similar to Taylor's equation (see chapter 3).

Blend	Interfacial tension (mN/m)	
	Palierne	Choi-Schowalter
H_{20}	1.255	2.069
H_{80}	1.408	2.197

Table 6.2: Interfacial tension values of uncompatibilised PP/HDPE blends

The interfacial tension values of PP/HDPE blends calculated from these equations are given in Table 6.2. In both cases, Palierne model gives lower values. It should be noted that in both methods, the blends show different α values, even though the difference is small. However, for a polymer blend system, it is believed that irrespective of the blend composition, the α should be the same. This slight difference between the α values arises from the parameter R_v, which is derived from the phase morphology. Note that since both the blends are not dilute systems, the average particle size (R_v) contains contributions from interfacial tension as well as coalescence effect. Thus the difference arises from the coalescence effect associated with R_v.

Blend	Interfacial tension (mN/m)	
	Palierne	Choi-Schowalter
H_{20}	1.255	2.069
H_{20}_0.5E1	0.327	0.611
H_{20}_0.5E3	0.165	0.272
H_{20}_0.5E5	0.157	0.258
H_{20}_0.5E10	0.181	0.297

Table 6.3: Effect of compatibilisation on the interfacial tension of H_{20} blends

Table 6.3 shows the effect of compatibilisation on the interfacial tension between the two components in H_{20} blends. On the basis of phase morphology studies (chapter 3), we concluded that addition of compatibiliser decreases the interfacial tension sharply up to CMC and beyond that a levelling off in interfacial tension occurs. Theoretical predictions of Noolandi and Hong, Leibler, Tang and Huang, Paul and Newman, etc. also support this fact. So based on the phase morphology, we expect a sharp decrease in interfacial tension with initial addition of compatibiliser up to CMC and thereafter a levelling off. It is obvious from the table that there is a very good correlation between the phase morphology and rheology since the interfacial tension calculated from storage modulus supported the morphological data. Note that addition of even 1wt% compatibiliser decreases α remarkably and this continues upto the CMC. Beyond CMC, the interfacial tension shows a levelling off and even slight increase is seen at higher compatibiliser concentration. Figure 6.8 presents a comparison between the morphology/ rheology data. There is a very good correlation between the particle size reduction (obtained from phase morphology) and interfacial tension reduction (calculated from rheology).

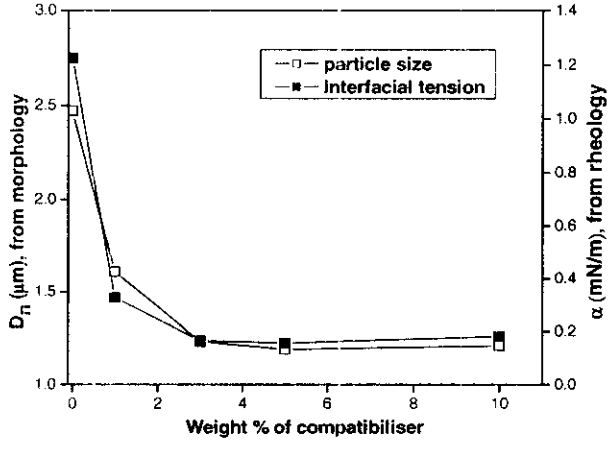

Figure 6.8: Comparison of particle size obtained from morphology and interfacial tension in the presence of compatibiliser

6.3. Conclusion

The present chapter was devoted to analyse the dynamic rheology of the blends as a function of blend ratio and compatibilisation. It was found that the complex viscosity of PP was maximum and that of HDPE was minimum. The complex viscosities of uncompatibilised blends were found to be intermediate. On the other hand the elastic properties of HDPE were found to be maximum where as those of PP were minimum.

Compatibilisation of the blends enhanced the complex viscosity of the blends. This was taken as an evidence for the compatibilising action of the blends. In contrary to our expectation, there was no true levelling off in rheological properties at CMC, but the rate of change in properties decreases beyond CMC. The interfacial tension of the blends in the presence and absence of compatibiliser was determined using Palierne method and Choi-Schowalter methods. Both the methods were successful and gave reasonably good values. The interfacial tension drastically decreased with the addition of compatibiliser up to CMC. It was also found that the minimum value was found at CMC and beyond that a levelling off is observed. Finally, a good correlation was made between the rheological properties and phase morphology.

6.4. References

1. L.A. Utracki, Commercial Polymer Blends; Chapman & Hall, London, (1998).

2. T. Araki, Q. Tran-Cong, M. Shibayama, Structure and Properties of Multiphase Polymeric Materials; Marcel Dekker Inc., New York, (1998).

3. S. Walheim, M. Ramstein, U. Steiner, Langmuir, **15**, 4828, 1999.

4. T. Matsumoto, N. Hori, M. Takahashi, Langmuir, **12**, 5563, 1996.

5. H.J. Kim, Y. Seo, Langmuir, **19**, 2696, 2003.

6. N.A. Frankel, A. Acrivos, Chem. Eng. Sci., **22**, 847, 1967.

7. W.R. Schowalter, C.E. Chaffey, H. Brenner, J. Colloid. Interface Sci., **26**, 152, 1968.

8. J.F. Palierne, Rheol. Acta, **29**, 204, 1990.

9. M. Loewenberg, E.J. Hinch, J. Fluid Mech., **321**, 395, 1996.

10. J.G. Oldroyd, Proc. Royal Soc., London, **A218**, 122, 1953.

11. S.J. Choi, W.R. Schowalter, Phys. Fluids, **18**, 420, 1975.

12. D. Graebling, D. Froelich, R. Muller, J. Rheol., **33**, 1283, 1989.

13. D. Graebling, R. Muller, J.P. Palieme, Macromolecules, **26**, 320, 1993.

14. H. Gramespacher, J. Meissner, J. Rheol., **36**, 1127, 1992.

15. B. Brahimi, A. Ait-Kadi, A. Ajji, R. Jerome, R. Fayt, J. Rheol., **35**, 1069, 1991.

16. M. Bousmina, P. Bataille, S. Sapieha, H.P. Schreiber, J. Rheol., **39**, 499, 1995.

17. C. Lacroix, M. Aressy, P.J. Carreau, Rheol. Acta, **36**, 416, 1997.

18. C. Lacroix, M. Girmela, P.J. Carreau, J. Rheol., **42**, 41, 1998.

19. Y. Germain, B. Ernst, O. Genelot, L. Dhamani, J. Rheol., **38**, 681, 1994.

20. C.J. Carriere, A. Cohen, C.B. Arends, J. Rheol., **35**, 205, 1991.

21. P. Scholz, D. Froelich, R. Muller, J. Rheol., **33**, 481, 1989.

22. H.S. Jeon, A.I. Nakatani, C.C. Han, R.H. Colby, Macromolecules, **33**, 9732, 2000.

23. J. Huitric, P. Mederic, M. Moan, J. Jarrin, Polymer, **39**, 4849, 1998.

24. I. Vinckier, P. Moldenaers, J. Mewis, J. Rheol., **40**, 613, 1996.

25. H. Asthana, K. Jayaraman, Macromolecules, **32**, 3412, 1999.

26. D. Shi, Z. Ke, J. Yang, Y. Gao, J. Wu, J. Yin, Macromolecules, **35**, 8005, 2002.

27. M. Bousmina, Rheol. Acta, **38**, 73, 1999.

28. E.V. Hemelrijck, P.V. Puyvelde, S. Velankar, C.W. Macosko, P. Moldenaers, J. Rheol., **48**, 143, 2004.

29. M. Minale, P. Moldenaers, J. Mewis, Macromolecules, **30**, 5470, 1997.

30. M. Minale, J. Mewis, P. Moldenaers, AIChE J., **44**, 943, 1998.

31. T. Jansseune, J. Mewis, P. Moldenaers, M. Minale, P.L. Maffettone, J. Non Newtonian Fluid Mech., **93**, 153, 2000.

32. I. Vinckier, H.M. Laun, Rheol. Acta, **38**, 274, 1999

33. Chr. Friedrich, W. Gleinser, E. Korat, D. Maier, J. Wees, J. Rheol., **39**, 1411, 1995.

34. A.Y. Coran, R. Patel, J. Appl. Polym. Sci., **20**, 3005, 1976.

35. W.G.F. Sengers, P. Sengupta, J.W.M. Noordermeer, S.J. Picken, A.D. Gotsis, Polymer, **45**, 8881, 2004.

36. S.H. Jafari, A. Yavari, A. Asadinezhad, H.A. Khonakdar, F. Bohme, Polymer, **46**, 5082, 2005.

37. B.D. Favis, in Polymer Blends, Volume 1, D.R. Paul, C.B. Bucknall, Eds., Wiley Interscience, New York, (2000).

38. S. Wu, Polymer, **28**, 1144, 1987.

39. P.H.P. Macaubas, N.R. Demarquette, Polymer, **42**, 2543, 2001.

40. Y.T. Sung, M.S. Han, J.C. Hyun, W.N. Kim, S.S. Lee, Polymer, **44**, 1681, 2003.

41. D. Graebling, R. Muller, J. Rhol., **34**, 193, 1990.

42. M. Bousmina, R. Muller, J. Rhol., **37**, 663, 1993.

43. P.J. Carreau, M. Bousmina, A. Ajji, in K.P. Ghiggin, Ed., Progress in Pacific Science-3, Springer-Verlag, New York, (1994).

44. C. Lacroix, M. Bousmina, P.J. Carreau, B.D. Favis, A. Michel, Polymer, **37**, 2939, 1996.

45. I. Delaby, B. Ernst, Y. Germain, R. Muller, J. Rheol., **38**, 1705, 1994.

46. U. Jacobs, M. Fahrlander, J. Winterhalter, C. Friedrich, J. Rheol., **43**, 1495, 1999.

47. N.W. Tschoegle, The Phenomenological Theory of Linear Viscoelastic Behaviour, Berlin, Springer, (1989).